JOURNAL OF CATALYSIS **175,** 316–327 (1998)
ARTICLE NO. CA971997

Isothermal Kinetic Study of the Decomposition of Nitric Oxide over Rh(111) Surfaces

Mansour Aryafar and Francisco Zaera[1]

Department of Chemistry, University of California, Riverside, California 92521

Received October 9, 1997; revised December 11, 1997; accepted December 11, 1997

The kinetics of the thermal decomposition of NO on Rh(111) surfaces was probed both by temperature-programmed desorption (TPD) experiments and by isothermal measurements using an extension of the so-called King and Wells collimated beam method. The TPD studies corroborated previously reported results, including the existence of two distinct N_2 desorption peaks, the first of which displays apparent first-order kinetics. The isothermal work proved that the adsorption of NO is precursor mediated at low temperatures, and that it is not affected significantly by the presence of coadsorbed nitrogen and/or oxygen atoms at any temperature below 900 K. The rate of molecular nitrogen production was found to be significant above 450 K and to be controlled by the recombination of atomic nitrogen below 600 K, but the experimental data could not be reproduced in a satisfactory manner by any empirical rate law unless the order in nitrogen coverage was set to be less than unity. Such an observation is interpreted here as being the result of the slow diffusion of nitrogen atoms across the surface prior to their recombination. A strong additional effect due to lateral repulsion between nitrogen and/or oxygen atoms was also inferred from the data. © 1998 Academic Press

1. INTRODUCTION

Air pollution originating from the exhaust of internal combustion engines has developed into one of the most serious environmental concerns in recent years, and nitrogen oxide emission control in particular has become one of the most important aspects of this problem being addressed in environmental regulations. The first limit on NO_x emissions from automobiles was set at 1 g/mile in 1981 (1, 2), but that value has been subsequently updated in later years, and the passage of the 1990 Clean Air Act Amendments and of many other regional laws is an indication that more regulations are quite likely to come in the near future (3, 4). The best answer to date to the problem of the removal of air pollutants from the emissions of automobiles is the use of the so-called three-way catalyst (2, 5), a combination of palladium, platinum, and rhodium particles deposited on high surface-area supports in which rhodium is used to reduce the nitrogen oxides produced during the combustion processes (6–9).

As a consequence of its importance in pollution removal, the reaction of NO on rhodium surfaces has been studied by using surface-sensitive techniques in some detail (10). On Rh(111), early temperature-programmed desorption (TPD) experiments were used to identify the N_2-producing channels (11). Interestingly, the desorption of that nitrogen was found to occur in two stages, around 470 and above 500 K. From these, the latter feature was determined to follow second-order kinetics, a fact that has been explained by assuming that the rate of reaction is controlled by the recombination of nitrogen atoms on the surface. The first peak, on the other hand, does not shift in temperature with changing coverages, a behavior generally associated with first-order processes. There has been quite a bit of speculation in the literature on the source of this low-temperature N_2 TPD peak. X-ray photoelectron spectroscopy (12), secondary ion mass spectrometry (SIMS) (12, 13), and vibrational spectroscopy (HREELS) (14, 15) have all been used to show that NO dissociation occurs at quite low temperatures, below 300 K at low coverages and around 450 K at high coverages. This observation led to the conclusion that such a reaction is not likely to be the rate-limiting step in the N_2 production, even though more recently it has been argued that it may still be relevant at high coverages, where the dissociation of the adsorbed NO is slowed down by the unavailability of empty surface sites (16). Another line of thought is based on the idea of a possible recombination of atomic nitrogen with adsorbed NO to form a N_2O-like intermediate under the conditions of the TPD experiments, but this has also been proven not feasible by a series of elegant isotope-labeling experiments with coadsorbed NO and nitrogen (17). Finally, kinetic simulations have been used to argue that the two nitrogen states can be explained by repulsive interactions among the atomic nitrogen and oxygen chemisorbed species (18–21), but since the same first-order N_2 TPD peak was shown to appear in experiments with pure nitrogen, where there is no oxygen on the surface to exert any effect on the reaction rates (16, 22),

[1] To whom correspondence should be addressed.

0021-9517/98 $25.00
Copyright © 1998 by Academic Press
All rights of reproduction in any form reserved.

other explanations may be needed to fully understand these processes.

In this paper we report isothermal kinetic experiments performed on the desorption and thermal conversion of nitric oxide over a Rh(111) surface. NO adsorption was found to go through a physisorbed precursor at low temperatures but to behave in a more Langmuir manner around room temperature. The initial sticking coefficient was shown to be quite high at all temperatures, as high as about 0.8 at 100 K, but to decrease slightly above 800 K. A couple of surprising additional facts were identified in these experiments as well. For one, the rate of nitrogen formation was seen to depend strongly on the surface coverages of both atomic oxygen and atomic nitrogen, but those species were proven to not affect the rate of NO uptake in any significant way. In addition, the yield for N_2 formation was seen to reach about 100% of the initial NO consumed at 450 K but to then decreases steadily at higher temperatures, even though the rates of NO consumption and nitrogen production follow identical behaviors with time above 600 K. These and other observations are discussed below in terms of possible kinetic models for the NO decomposition process.

2. EXPERIMENTAL

All the experiments reported here were performed in a 6.0 L stainless steel ultrahigh vacuum (UHV) chamber evacuated with a 170 L/s turbo-molecular pump to a base pressure of about 2×10^{-10} Torr and equipped with a UTI 100C quadrupole mass spectrometer, a sputtering ion gun, and a molecular beam doser. Detailed descriptions of the doser setup and of its calibration have been given elsewhere (23, 24). Briefly, the doser, a 1.2 cm diameter array of parallel microcapillary glass tubes, is connected to a calibrated volume via a leak valve and a second shutoff valve that isolates it from the main vacuum vessel. The beam flux is set by filling the backing volume to a specific pressure, which is measured by a MKS baratron gauge, and by adjusting the leak valve to a predetermined setpoint. A movable stainless steel flag is placed between the sample and the doser in order to intercept the beam at will.

The sample, an approximately rectangular (1.10 cm $\times$ 0.56 cm) Rh(111) single crystal, was cleaned *in situ,* initially by Ar^+ sputtering and before each experiment by cycles of oxygen exposures (1×10^{-7} Torr for up to 20 min) at 900 K and annealing to 1200 K until the NO TPD spectra reported in the literature (11, 13) could be reproduced. The crystal was placed at a distance of 0.5 cm from the front of the doser to assure a reasonably flat gas flux profile (23), and heated resistively and cooled by using a liquid nitrogen reservoir. The surface temperature was monitored continuously by a chromel–alumel thermocouple spot-welded to the back of the crystal, and kept constant during the kinetic runs with a homemade precision temperature controller. TPD spectra were recorded at a heating rate of about 10 K/s. Both the regular NO (Liquid Carbonic, >99.99% purity) and the isotopically labeled ^{15}NO (CIL, 98% ^{15}N purity) were used as supplied. The pressures of the gases during the dosing experiments done by backfilling of the chamber were measured with a nude ion gauge and were then calibrated for differences in ionization sensitivities (25).

The time evolution of the partial pressures of up to ten different species was followed in both the isothermal kinetics and the TPD experiments by using the quadrupole mass spectrometer, which was placed out of the line of sight of the beam and the crystal in order to avoid any artifacts due to possible angular profiles in either the scattered or the desorbing gases, and which was interfaced to a personal computer. The mass spectrometer signal for nitric oxide was calibrated by equating the time-integrated NO uptake on clean Rh(111) at 100 K to its saturation coverage, which was assumed to be about 0.70 monolayers (ML) (11–13, 15, 26). The N_2 signal was then calibrated by using the relative mass spectrometer sensitivities for NO and N_2 and independently by using mass balance arguments and assuming a constant sticking coefficient in TPD experiments.

3. RESULTS

3.1. General Results

Figure 1 displays the series of TPD traces obtained here for NO on Rh(111) as a function of initial coverage. ^{15}N-labeled nitric oxide was used to separate any possible contributions from background CO to the signal of the nitrogen-containing compounds, even though CO desorption was also monitored and shown to not interfere with the chemistry reported here. Only molecular ^{15}NO (31 amu) and $^{15}N_2$ (30 amu) were detected in these experiments, no $^{15}N_2O$ was observed in any case, and the traces registered in our study were found to match quite nicely those reported previously (11, 13). Molecular nitric oxide desorption is not seen at low exposures, only above 0.6 L a peak develops around 440 K in a peak that then grows but does not shift with increasing initial NO doses, a behavior characteristic of first-order kinetics. In addition, a low-temperature shoulder also grows at high coverages. In terms of nitrogen desorption, a second-order peak appears right from the beginning of the uptake. That feature peaks around 700 K for 0.2 L of NO but shifts significantly toward lower temperatures with increasing NO doses until saturating about 0.6 L, at which point it reaches its maximum at 560 K. A second feature then develops about 460 K and grows without shifting until reaching saturation at approximately 3.0 L of NO. The inset in Fig. 1 displays the overall ^{15}NO and $^{15}N_2$ yields versus initial ^{15}NO exposure as calculated by integration of the respective TPD traces.

Isothermal NO uptake experiments were also performed for different temperatures ranging from 100 to 900 K. In

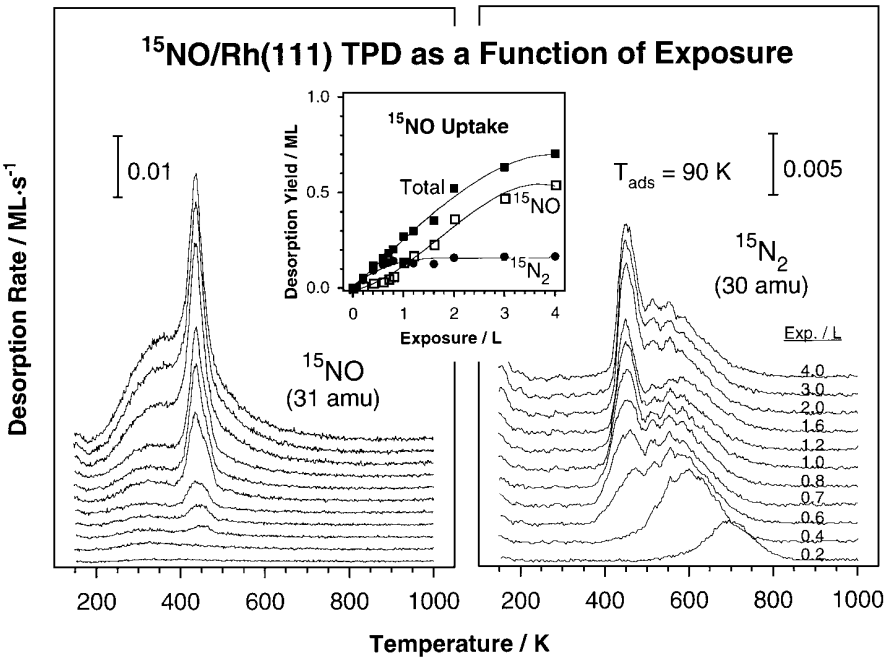

FIG. 1. ^{15}NO (31 amu, left panel) and $^{15}N_2$ (30 amu, right panel) TPD spectra from ^{15}NO adsorbed on Rh(111) at 90 K as a function of initial dose. Heating rates of 10 K/s were used in all experiments. The inset displays the coverage dependence of the total yields as calculated by using the areas under the TPD traces. Of particular relevance to this report is the appearance of two peaks in the molecular nitrogen TPD traces, one above 500 K which is seen at all coverages and displays second-order kinetics, and a second that grows after exposures above 0.6 L and peaks at 460 K irrespective of coverage, a behavior usually associated with first-order kinetics.

view of the similarity between the TPD results obtained with normal and isotopically labeled NO, normal ^{14}NO was used in the rest of the studies reported here. The left panel of Fig. 2 shows a typical example (in this case for a surface temperature of 450 K) of the raw data obtained in the isothermal experiments. Although only the traces for NO (30 amu) and N_2 (28 amu) are shown here, several other key masses were followed as well, including 12 (C),

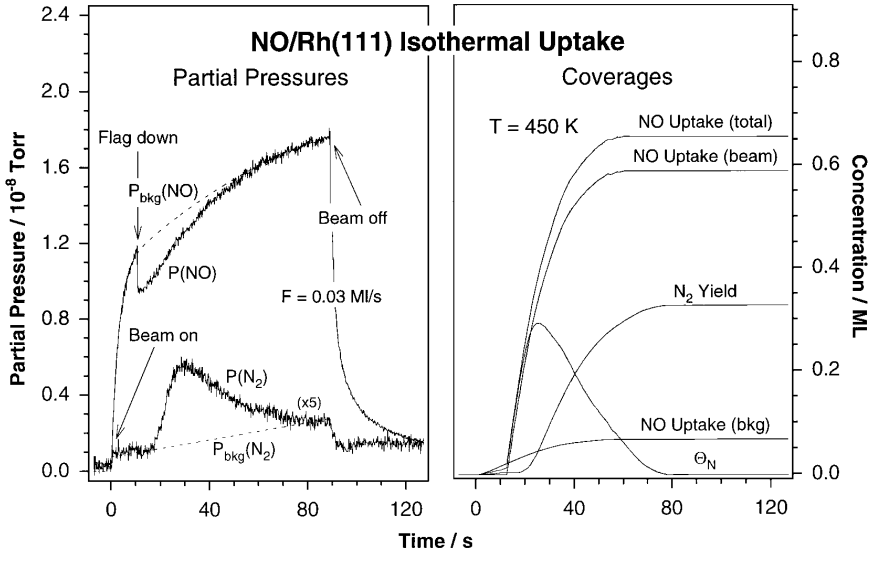

FIG. 2. (Left) Typical raw data from an isothermal kinetic run of the type described in this report. An effusive collimated NO molecular beam is directed onto a Rh(111) surface, which is kept at a constant temperature (450 K in this example), and the evolution of the partial pressures of NO and N_2 is followed versus time. The NO flux in all the experiments reported here was calibrated and set to a value of 0.03 ML/s. (Right) Time evolution of the NO uptake both from the beam and from the background gases, of the N_2 evolution, and of the surface coverage of nitrogen atoms during the same experiment. The coverages and yields were calculated by integration of the raw data as described elsewhere (23, 27).

14 (N), 16 (O), 32 (O_2), and 44 (N_2O and CO_2) amu; no additional features were seen in those data. The experimental details and data analysis have been described in detail elsewhere (23, 27), so they will only be described briefly here. The experimental sequence in each run was as follows: (i) the beam, which was set to a flux of about $F = 0.03$ ML/s, was turned on at time $t = 0$, at which point an increase in the NO background pressure was observed; (ii) the NO partial pressure was allowed to reach its new steady-state value by waiting for about 10 s, after which the intercepting flag was removed in order to allow the beam to impinge directly on the rhodium crystal. This caused a drop in NO partial pressure related to the uptake of NO on the surface which continued until the crystal became saturated; (iii) finally, after about 80–100 s, the beam was turned off and the vacuum chamber was allowed to reach its base pressure again.

The raw data from the isothermal experiments could be easily converted into surface coverages, reaction yields, and reaction rates after appropriate calibrations (23, 27). The temporal evolution of both the key surface coverages and the yield of molecular nitrogen for the example in Fig. 2 is presented in the right panel of that figure. A few points are worth highlighting here. First, the geometrical arrangement of our experiment is such that only about 30% of the beam is intercepted by the crystal, hence the relatively shallow drop in pressure when the flag is removed; this is done by design to ensure that the beam profile is approximately constant across the surface of the crystal (23). Second, the partial pressure of NO in the chamber increases (to about 1.0×10^{-8} Torr in the experiments reported here) right after the beam is turned on, and that induces some additional NO adsorption not accounted for in the analysis of the uptake from the direct beam. We always include this background adsorption in our calculations, even though it amounts to less than 10% of the total adsorption (see the right panel of Fig. 2). Third, because the pumping speed for nitric oxide in the chamber is poor, the partial pressure of that gas never equilibrates but increases steadily during the kinetic runs instead. To estimate the time dependence of the equilibrium pressure, which is needed to calculate coverages and rates, a combination of an exponential and a quadratic equation was fitted to the points before and after NO adsorption from the direct beam; this functional form was tested by making sure that it fitted the results from reference experiments where the flag was never removed from the path of the beam. The results of this background adjustment, illustrated by the broken line displayed in Fig. 2, were quite satisfactory in all cases. Fourth, simple stoichiometric arguments were used to estimate the coverages of the surface species, including the assumption that at least above 400 K all initial NO dissociates rapidly to atomic nitrogen and atomic oxygen (13–15); the surface coverage of the molecular nitric oxide was considered to be close

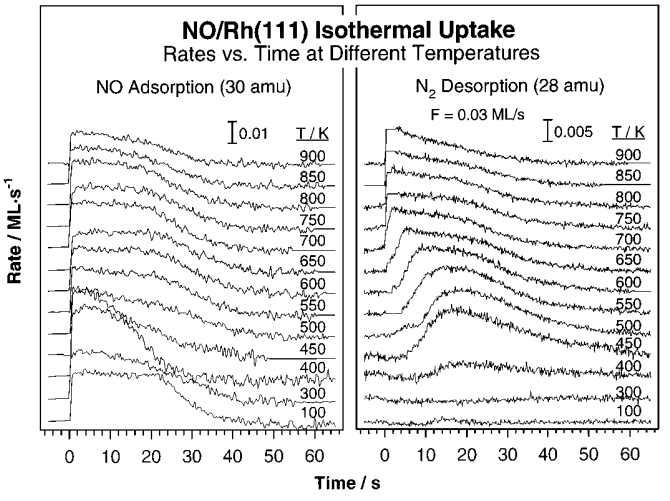

FIG. 3. Time evolution of the NO adsorption (30 amu, left) and N_2 desorption (28 amu, right) rates during kinetic experiments such as that described in Fig. 2 for different surface temperatures. Three clear temperature regimes were identified in these experiments: (i) below 400 K, where no reaction takes place; (ii) above 700 K, where the rate of N_2 production is limited by the impinging frequency of NO on the surface; and (iii) between 400 and 700 K, an intermediate region with complex kinetic behavior.

to zero at all times during the runs in the high-temperature cases. Finally, note that in the particular example illustrated here almost all the atomic surface nitrogen recombines to produce nitrogen gas: the fact that the N_2 yield can never exceed half of the NO total uptake provides a further way to check both the background subtraction and the calibration of the relative sensitivities of the mass spectrometer.

Figure 3 displays the temporal evolution of the rates of NO consumption (30 amu, left panel) and N_2 desorption (28 amu, right panel) during the isothermal uptake of NO on Rh(111) at different crystal temperatures. The time scale has been shifted here to set $t = 0$ at the point where the beam is allowed to impinge directly on the crystal. From the data in this figure it can be seen that, first of all, the initial rate of NO adsorption is approximately constant in all cases, and that it is limited by the beam flux and the NO initial sticking coefficient, which is about 0.7–0.8 (see below). Also, three distinct temperature regimes can be distinguished: (i) below 400 K, where NO adsorption is not accompanied by any N_2 production; (ii) between 400 and 700 K, where nitrogen production is delayed and displays a kinetic behavior different to that seen for NO consumption; and (iii) above 700 K, where the time evolution of the rates of NO uptake and N_2 desorption display identical trends. An early feature was seen in the 28 amu trace above 500 K due to CO formation from recombination between oxygen from NO decomposition and carbon segregating from the bulk. This was clearly determined by the observance of matching features in the 12 and 16 amu traces and the absence of such peaks in the 14 amu data, and was removed from all but the 500 K trace.

The three temperature regimes identified above will be discussed in more detail in the following paragraphs.

3.2. NO Adsorption below 400 K

As mentioned above, NO adsorption on Rh(111) surfaces is molecular below room temperature and does not lead to any nitrogen gas formation. The uptake kinetics does nevertheless change significantly with temperature. Figure 4 displays the dependence of the NO sticking coefficient on surface coverage for 100 and 300 K. The initial sticking coefficient is approximately the same in both cases, about 0.75, but while the adsorption probability remains almost constant throughout most of the uptake in the 100 K case, it decreases significantly with coverage at 300 K. The behavior at liquid nitrogen temperatures is typical of precursor-mediated adsorption: the early part of the 100 K trace can be fitted to a Kisliuk-type equation (28) by assuming a ratio between the rate of desorption from the precursor state and that of surface migration of about $K = k_{des}/k_{mig} = 0.03$. The fit does deviate from the experimental data at coverages above about 0.5 ML, perhaps because of the presence of two types of adsorption states on the surface (29). The kinetics observed at 300 K, on the other hand, is more like that expected by Langmuir's model; the Kisliuk equation yields a value of $K \approx 0.2$. This provides an estimate for the difference in activation energies between desorption and migration from the physisorbed state of about 0.5 kcal/mol.

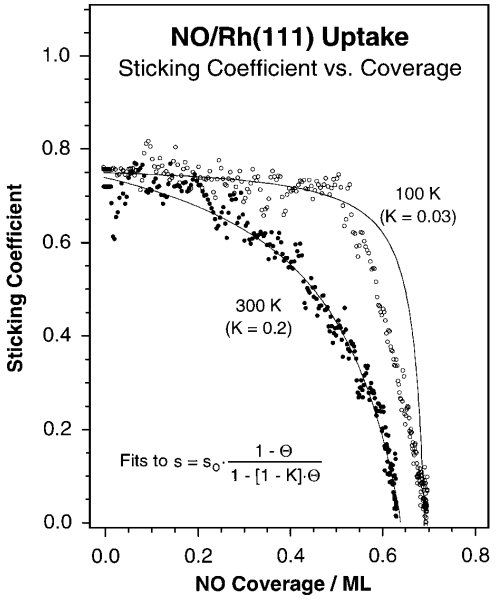

FIG. 4. Sticking probability (s) vs NO coverage for the adsorption of NO on Rh(111) at 100 and 300 K. The initial sticking coefficient is quite high (about 0.75) at both temperatures. However, while the uptake at low temperatures displays the approximately constant s value with coverage typical of precursor-mediated adsorption kinetics, that at 300 K resembles more closely a Langmuir-type behavior.

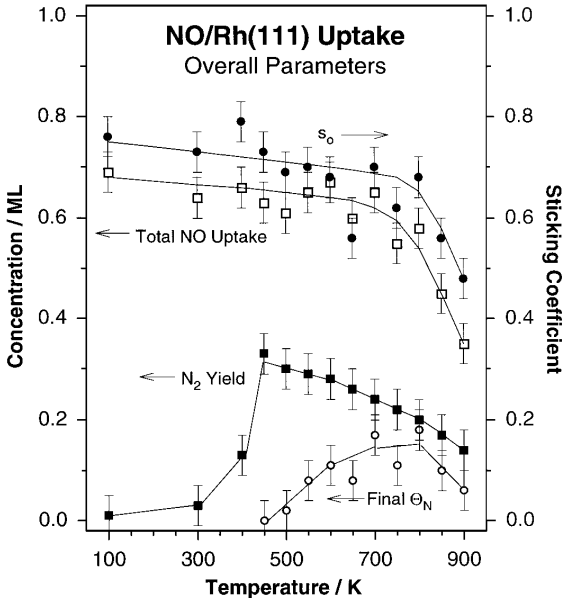

FIG. 5. General kinetic parameters obtained from the isothermal runs shown in Fig. 3 for the adsorption and thermal conversion of NO on Rh(111) as a function of surface temperature. Shown are values for the initial NO sticking probability (s_0), the total NO uptake, the overall N_2 yield, and the coverage of the atomic nitrogen that remains on the surface after the experiments (Θ_N). A few observations become evident from the data in this figure: (i) both s_0 and the total NO uptake remain almost constant between 100 and 800 K; (ii) the nitrogen yield starts to be significant only above 400 K and peaks about 450 K before gradually decreasing again; and (iii) some residual nitrogen atoms are left on the surface after the kinetic runs performed at temperatures above 500 K.

The data in Fig. 3 can also be used to calculate initial sticking coefficients and overall yields as a function of surface temperature. Those are summarized in Fig. 5. Among the results worth highlighting here we can mention the following three points. (i) The initial sticking coefficient for NO is quite high, between 0.7 and 0.8, and remains approximately constant with temperature until about 800 K, at which point a sudden drop in value is observed. (ii) The total uptake of NO also remains almost constant over the same temperature range, even though complete dissociation and nitrogen desorption is seen above 400 K. This suggests that NO adsorption is basically unaffected by the presence of atomic nitrogen and atomic oxygen on the surface (more on this later). (iii) The yield for nitrogen production peaks around 450 K, at which point it is almost quantitative, but then decreases slowly with increasing temperature until accounting for only about $\frac{2}{3}$ of the total nitrogen consumed above 800 K.

3.3. Kinetics of NO Decomposition on Rh(111) between 400 and 700 K

Above 400 K the formation of nitrogen gas becomes evident in the data shown in Fig. 3. Also clear from those data is the fact that the kinetics of the N_2 desorption display

a behavior quite different to that of the NO adsorption. Perhaps one of the most interesting features in the temporal behavior of the N_2 production in this temperature regime is the delay observed between the beginning of the NO uptake and the onset of nitrogen detection. This delay appears to correspond to the buildup of a critical nitrogen concentration which roughly matches that seen in the high-temperature N_2 peak in the TPD data, but in fact the atomic nitrogen coverage at which N_2 starts to be produced changes with temperature, decreasing monotonically as the reaction is performed on hotter surfaces. Indeed, while Θ_N approaches 0.2 ML before any significant N_2 production is detected at 450 K, that threshold value is already cut by half at 600 K. Such continuous changes in critical nitrogen coverage with temperature argue against any idea based on the existence of more than one type of kinetically different nitrogen atoms on the surface. Two explanations have been discussed in the past in connection with the complex kinetic behavior for nitrogen production from NO on Rh(111), namely, competition between NO dissociation and nitrogen recombination rates in this low-temperature regime, and lateral interactions among the different species adsorbed on the surface, especially between nitrogen and oxygen.

Assuming that NO dissociation is rate limiting alone cannot explain the kinetic behavior observed here. This can be tested with the data in Fig. 6, which displays the rate of nitrogen production $R(N_2)$ as a function of the coverage of nitrogen atoms Θ_N for different surface temperatures. Here the data are shown in a way to highlight the fact that there is no linearity between the logarithm of the rates and the logarithm of the coverages, an indication that the rate of nitrogen production is not proportional to the coverage of nitrogen to a fixed exponent. Five things become evident from these data: (i) there is a sudden rise in the N_2 production rate but only after reaching the critical nitrogen coverage on the surface discussed before; (ii) as also mentioned above, the critical N coverage becomes smaller at higher temperatures; (iii) the subsequent leading edge is quite steep in all cases, having slopes on the order of 4–6, too high to have any physical meaning in terms of orders in reaction rate laws; (iv) for the same nitrogen coverage, the reaction rates are quite different in the rising and trailing edges of the kinetic experiments, that is, the rates for nitrogen desorption at a given Θ_N are much higher after longer reaction times, presumably because of the enhancing effect exerted by the coadsorbed oxygen left behind on the surface after NO dissociation; and (v) the rate of nitrogen desorption in the trailing side of the isothermal kinetic runs is approximately proportional to the coverage of nitrogen on the surface at low temperatures, but its behavior becomes more complex above 550 K. There is in fact a clear change in the kinetic behavior of this system around that temperature, since below 550 K the nitrogen coverage

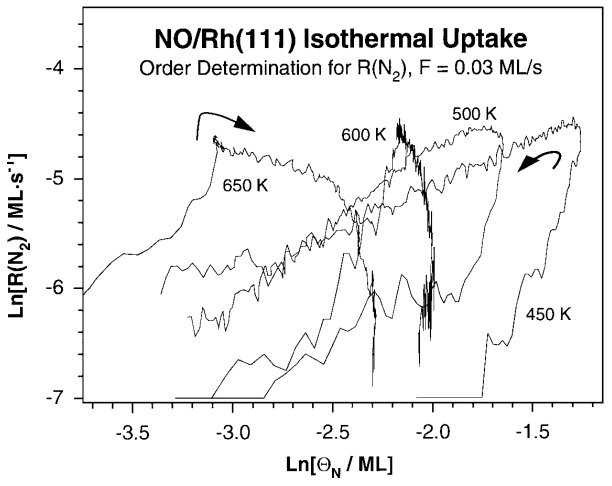

FIG. 6. Molecular nitrogen production rate as a function of atomic nitrogen surface coverage during isothermal kinetic runs performed at several surface temperatures between 450 and 650 K. The data are shown in a log–log fashion in order to highlight possible empirical reaction rate orders. The arrows indicate the temporal sequence of the data acquisition. The things to notice here are (i) the N_2 desorption only starts after the buildup of a critical N surface concentration, but that Θ_N decreases as the reaction temperature is increased; (ii) initially the N_2 production rate grows quite steeply, especially at low temperatures, and then reaches a maximum (the same as Θ_N) between 450 and 550 K; (iii) the reaction rate during the trailing edge of the experiment decreases in a slower manner, and does not match the values seen for the same nitrogen coverages during the initial uptake; and (iv) the trailing edge kinetics can be empirically described by a rate law where the N_2 desorption rate is roughly proportional to Θ_N at temperatures below 550 K.

reaches a maximum before decreasing again in the latter part of the runs, but above 600 K this is no longer the case. It is interesting to notice that the 550 K split corresponds roughly to the dividing temperature between the two N_2 peaks in the TPD experiments (see Fig. 1).

One thing that is clear from Fig. 6 is that the oxygen atoms codeposited during the NO decomposition greatly influence the rate of nitrogen gas production. The quantification of this effect, however, is not straightforward. It could be argued that the nitrogen and oxygen atoms compete for the same adsorption sites on the surface. If each of those types of atoms clusters in islands on the surface, as recent STM experiments suggest (30), this would mean that the coadsorbed oxygen effectively increases the local coverage of nitrogen on the surface (by blocking surface patches and consequently reducing the surface area available for the N atoms). One way to test this hypothesis is to check the dependence of the reaction rates on either the total (N + O) coverage or an effective nitrogen surface concentration calculated by scaling the available sites after subtracting those used by oxygen atoms. Several attempts were made here to fit the data to such parameters, some of which are illustrated in Fig. 7. It was again found that none of these assumptions is by itself sufficient to account for

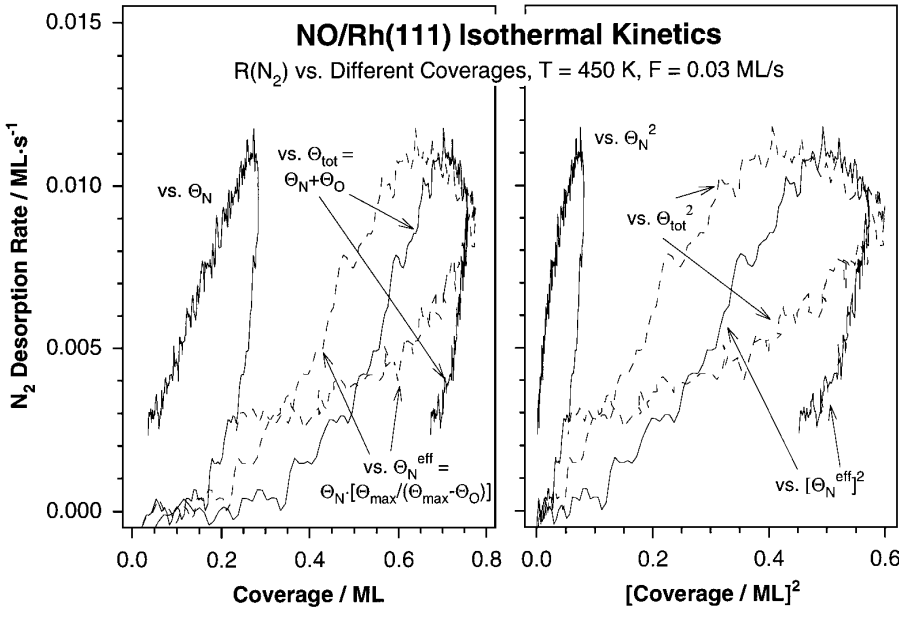

FIG. 7. Evolution of the molecular nitrogen production rate at 450 K plotted against different coverages to aid in the understanding of the mechanism for the overall reaction. The left panel shows the rate data plotted against the coverage of atomic nitrogen on the surface (Θ_N), the combined coverages of atomic oxygen and nitrogen ($\Theta_N + \Theta_O$), and an effective nitrogen coverage calculated by scaling the total number of sites available after taking into account the blocking effect of oxygen (see text for details). The right panel displays the same data versus the square of those coverages to test the validity of a straight second-order rate law. None of the traces can be associated with a simple rate expression.

the kinetic behavior in the isothermal kinetic experiments, in part because $R(N_2)$ eventually decreases in spite of the continuous buildup of oxygen atoms on the surface.

Another aspect of the behavior of the NO/Rh(111) system highlighted by our studies is the fact that the kinetics of NO adsorption is not affected significantly by the buildup of adsorbates on the surface, and that therefore it must not play an important role in determining the overall kinetics of this system below 550 K. In fact, the NO uptake is controlled by the impinging flux throughout most of the kinetic runs reported here. This can be seen by the approximately constant nature of the NO consumption rate up to high N + O coverages, as observed in the plots of R(NO) vs $\Theta_N + \Theta_O$ shown in Fig. 8. In addition, N_2 production is seen only above 450 K, a temperature higher than that needed to dissociate chemisorbed NO on Rh(111) (13, 18, 29). This means that in the relevant isothermal experiments the nitric oxide molecules break apart immediately after adsorption, which means that the steady-state NO surface concentration remains low at all times. Notice, finally, that the shape of the trailing edge of the $R(N_2)$ curves match those of R(NO) above 550 K, suggesting that the kinetics of nitrogen formation is limited by the impinging frequency of the incoming NO molecules in that temperature regime.

An attempt was made to reproduce the kinetic data in the 450–550 K range by a series of mathematical equations, but no fit was found to be entirely satisfactory. Among the unsuccessful hypothesis tested here we can cite the following:

(i) The limiting step is the dissociation of NO. The rate constant was calculated accordingly by dividing the rate of nitrogen desorption by the coverages of NO (calculated by integration of the uptake assuming negligible dissociation) and empty sites. It was found that this constant increases monotonically with increasing oxygen surface coverage, from about zero at the start of the run, to a value of approximately $0.4\,(\mathrm{ML}\cdot\mathrm{s})^{-1}$ toward the end. It also became quite clear that adding a factor for the coverage of empty sites to any rate expression only led to further deviations from the experimental data, because such Θ_{empty} term is always higher at the beginning of the kinetic runs where the induction period is observed. In any case, given that there is ample evidence for NO dissociation below 400 K, especially at low coverages (12–14), this model was not pursued any further.

(ii) The limiting step is the recombination of nitrogen surface atoms. This assumption by itself is not capable to account for the behavior reported here, as discussed earlier. The reaction rate constant calculated by dividing $R(N_2)$ by Θ_N^2 varies by more than an order of magnitude throughout each kinetic run.

(iii) The recombination rate is affected by the presence of nitrogen and oxygen atoms on the surface. The rate constants calculated in (ii) were fitted to a couple of equations to account for this effect: (a) one with an exponential term that included linear components dependent on the coverages of oxygen and nitrogen, as reported by Belton *et al.* (16), and (b) a more sophisticated expression based on a

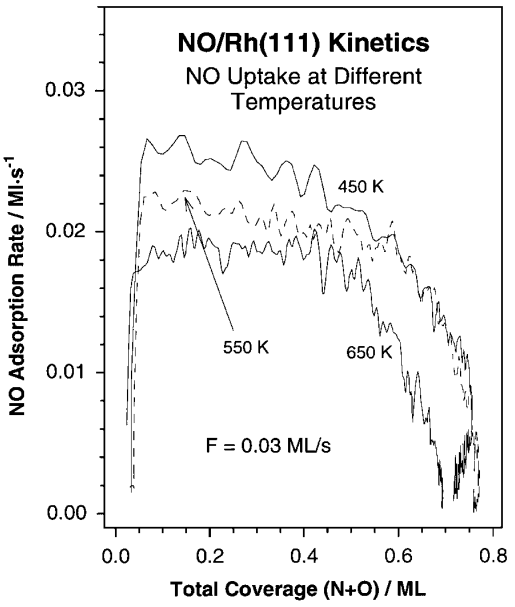

FIG. 8. NO uptake kinetics during isothermal kinetic runs at temperatures between 450 and 650 K. The rate of NO adsorption, R(NO), plotted here against the combined coverages of oxygen and nitrogen atoms, remains almost constant up to quite high $\Theta_N + \Theta_O$ coverages in all cases, indicating that the initial NO adsorption step is limited by the availability of NO molecules from the gas phase under the conditions of the experiment, and that therefore the NO uptake does not control the kinetics of N_2 production below 600 K.

lattice gas model for well-mixed adlayers, as suggested by Makeev *et al.* (19). No good fits were obtained in either case.

(iv) The nitrogen and oxygen atoms segregate and form islands on the surface. This has in fact been reported to occur at room temperature, as seen by STM experiments (30). In order to include this effect, the surface was in effect partitioned between the oxygen and the nitrogen, and the nitrogen coverage was scaled by the fraction allotted to the N atoms. This was done in one of two ways, the same as in Fig. 7: (a) by using the expression $\Theta_N^{\text{eff}} = \Theta_N[(\Theta_N + \Theta_O)/\Theta_N] = \Theta_N + \Theta_O$ and (b) by employing the equation $\Theta_N^{\text{eff}} = \Theta_N[\Theta_{\max}/(\Theta_{\max} - \Theta_O)]$. In each case new rate constants were calculated with the expression $k = R(N_2)/(\Theta_N^{\text{eff}})^2$, and those were fitted to the two models described in (iii) (but considering lateral interactions with other nitrogen atoms only). None of these attempts was successful either.

The best results were obtained by relaxing the requirement of the process being second order in nitrogen coverage. In order to include the reaction order as a parameter and still keep the number of parameters to a minimum, an additional assumption was made here, namely, that the lateral interactions among nitrogen and oxygen atoms are all of a comparable magnitude. It was also found that, everything else equal, better fits were obtained by using Θ_N instead of either of the Θ_N^{eff} described above, a result that in effect implies that the O and N atoms are likely to intermix and not segregate at the temperature of the reactions. The best least-squares fit to the data for 450 K using this simple three-variable model yielded the following equation (Fig. 9):

$$R = (7.6 \times 10^{-4})(\Theta_N)^{0.71} \exp[4.9(\Theta_N + \Theta_O)].$$

This corresponds to an empirical rate law where the reaction order with respect to the coverage of nitrogen is 0.71 and the average repulsive energy between nitrogen and oxygen atoms is about 5.4 kcal/(mol · ML). It is important to point out that the fitting of the experimental data to this type of equation, which is by no means ideal at 450 K, becomes worse as the reaction temperature is increased, presumably because the overall reaction rate starts to become limited by the availability of NO molecules.

3.5. NO Decomposition Kinetics above 700 K

The kinetic behavior of the NO/Rh(111) system becomes somewhat simpler at higher temperatures. The nitrogen coverage threshold above which nitrogen gas production starts becomes smaller, to the point of being undetectable by 650 K. Furthermore, the rate of N_2 desorption becomes proportional to the rate of NO consumption in the trailing edge of the kinetic runs at temperatures as low as 600 K, as mentioned earlier. Interestingly, though, the proportionality constant between the two rates comes out to be about 0.35, that is, $R(N_2) = 0.35R(NO)$, not 0.5 as expected on stoichiometric grounds (see Fig. 10). This means that not

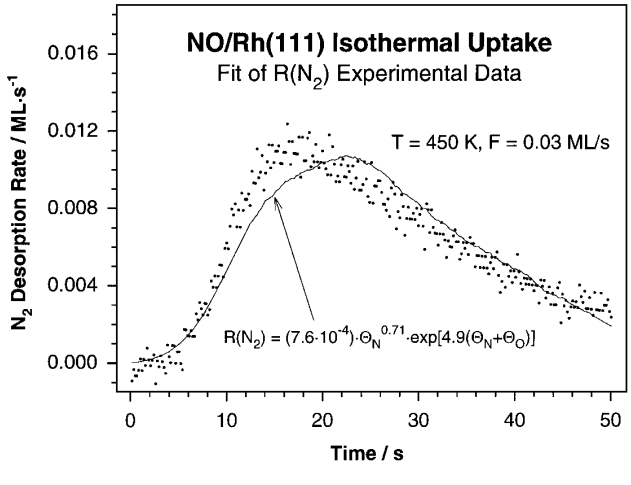

FIG. 9. Best least-squares fit of the N_2 production rate experimental data at 450 K (dots) to an equation of the form indicated in the figure (solid line). Several models were used to try to reproduce the experimental data, but no acceptable fit was possible unless the order of the reaction was allowed to become less than unity, a fact that suggests nitrogen atom diffusion on the surface as the limiting step in the overall NO conversion to N_2. An additional term was also added to account for the strong repulsive interactions between adsorbed nitrogen and/or oxygen atoms.

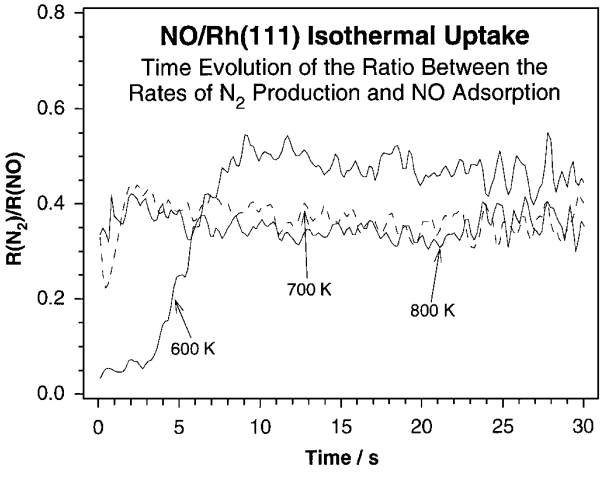

FIG. 10. Temporal evolution of the ratio between the rates of N_2 production and NO adsorption during isothermal kinetic runs at temperatures between 600 and 800 K. The constant nature of that ratio throughout the runs is indicative of the rate-limiting nature of the NO impinging frequency on the surface. Interestingly, though, a value of about 0.35 was obtained for $R(N_2)/R(NO)$ above 650 K, well below the 0.5 number expected on stoichiometric grounds.

all of the nitrogen atoms on the surface recombine to form N_2; about 25–30% remain on the surface long after the NO uptake becomes undetectable. It is tempting to doubt the calibration procedure used to estimate the sensitivity differences for N_2 and NO, since a 30% change in that number would produce the 0.5 stoichiometric factor mentioned above. Two arguments can be put forward against this objection: (i) the sensitivity calibration was done independently by two methods, by using the known reported values, and by mass balancing the products observed in TPD; and (ii) the proposed change would lead to N_2 yields above 100% at lower (450–550 K) temperatures. Notice the almost stoichiometric character of the reaction at 450 K, as shown in Figs. 2 and 5.

The other interesting behavior to be highlighted in this high-temperature regime is the steady decreases in sticking coefficient and overall conversion yield seen in Fig. 5. The initial sticking coefficient s_0 goes from approximately 0.7 below 700 K to less than 0.5 at 900 K, and the total amount of NO consumed decreases from over 0.6 to about 0.35 ML. The reduction in the apparent sticking probability could be accounted for by a lesser ability for the incoming molecules to accommodate their excess energy, but the fact that the overall uptake decreases as well favors an alternative explanation based either on a relative increase in NO desorption rate or on a decrease in the NO decomposition probability induced by the rearrangement of the atoms present on the surface. Related to this is the fact that above 500 K some nitrogen is always left behind on the surface after the reaction is complete (Fig. 5), an observation that is difficult to understand when focusing on the NO dissociation and nitrogen recombination kinetics alone but that may be explained by considering the diffusion of N atoms into the bulk of the rhodium sample.

4. DISCUSSION

The isothermal kinetic experiments reported above provide new insights on the mechanism for the thermal decomposition of nitric oxide on Rh(111) surfaces. Previous research in this field has led to the identification of the main elementary steps involved in this system:

$$\mathrm{NO(g)} \leftrightarrow \mathrm{NO(ads)}, \quad [1]$$

$$\mathrm{NO(ads)} \rightarrow \mathrm{N(ads)} + \mathrm{O(ads)}, \quad [2]$$

$$\mathrm{2N(ads)} \rightarrow \mathrm{N_2(g)}, \quad [3]$$

$$\mathrm{2O(ads)} \rightarrow \mathrm{O_2(g)}. \quad [4]$$

From these, oxygen recombination (step 4) is known to occur only above 1000 K (11), at temperatures much higher than those used in most studies, so no more will be said about that reaction here. Also, any additional steps involving the possible recombination of nitrogen atoms with NO molecules have already been shown to not be important under UHV conditions (17).

The seemingly simple mechanism given above hides several complications which have not been resolved to date. In particular, TPD experiments with NO on Rh(111) display two distinct N_2 desorption peaks (11, 13). The first peak (sometimes called β_2 or β-N_2), which is seen in all the TPD traces, has a maximum about 700 K at low coverages, and shifts significantly toward lower temperatures with increasing surface concentration, a behavior typical of second-order kinetics. The second feature (referred in the literature as either the β_1 or the δ-N_2 state), on the other hand, develops after NO coverages above 0.2 ML and peaks about 460 K but does not shift with coverage, a behavior typically associated with first-order kinetics. Molecular NO desorption is also seen at coverages above about 0.2 ML (approximately a third of saturation), and peaks around 440 K, a temperature about 20 K lower than that seen for the β_1 state of N_2.

The kinetic behavior of the β_1 nitrogen peak was explained early on in terms of a reaction between adsorbed nitrogen atoms and NO molecules to produce a N_2O or related intermediate (11). Such an idea can be made consistent with the first-order kinetics derived from the TPD data, but it cannot explain the lack of isotopic mixing in the N_2 produced in experiments with mixtures of normal and ^{15}N-labeled nitric oxide (17). An alternative explanation has been proposed where the first-order nature of the β_1 peak is associated with the fact that N_2 production below 500 K is limited by the previous NO dissociation step (13, 17). Again, several arguments can be put forward to

argue against this model. In particular, NO dissociation has been shown by XPS (12) , SIMS (12, 13), and HREELS (14, 15) to always occur below 400 K (and as low as 250 K at low coverages), temperatures well below those at which a detectable production of molecular nitrogen was seen in the isothermal kinetic runs reported here. At this point it is important to make a distinction between isothermal and TPD experiments, because it has been clearly shown before that the rate of NO dissociation on rhodium is inhibited by an increase of its coverage on the surface. This has some implications for the TPD data and could explain, at least in part, the nature of the β_1-N_2 peak. In the isothermal experiments reported here, however, the NO molecules dissociate as they adsorb, so no buildup of molecular species is expected at surface temperatures above the reaction threshold value (about 400 K). Indeed, recent time-dependent SIMS experiments done under conditions similar to those used in this work have shown that NO dissociation is so fast at 450 K that molecular species are not observed on the surface at any point during the uptake (29). In any case, no kinetic model involving the rate of NO dissociation could be fit to any of the data in Fig. 3.

A direct conclusion from the work reported in this paper is the fact that the rate of NO adsorption is not affected in any significant way by the presence of nitrogen and/or oxygen atoms on the surface between 100 and 900 K (see, for instance, the data in Figs. 5 and 8). Consequently, the first step in the mechanism summarized above cannot account for the kinetic behavior of nitrogen production in the crucial temperature regime, between 400 and 600 K, either; only above 600 K does $R(N_2)$ match $R(NO)$ (Fig. 10). This leaves one remaining possibility, namely, that the atomic nitrogen recombination step controls the kinetics of gaseous molecular nitrogen formation in both of the temperature regimes defined by the two peaks in the N_2 TPD. That is not to say that invoking a simple bimolecular step is sufficient to account for the body of TPD and isothermal kinetic data available on this system to date. On the contrary, what this means is that a complete explanation of the kinetics of this system requires a more detailed analysis of the characteristics of the surface reaction at a molecular level.

One thing that has been pointed out in previous work and that has become evident in the kinetic studies reported here is the fact that the oxygen atoms codeposited during the NO decomposition reaction exert a profound effect on the rate of the surface nitrogen recombination step. This is clearly visible in the data shown in Figs. 6 and 7, where the rate of N_2 production for a given atomic nitrogen coverage is shown to be significantly different during the early and later parts of the kinetic runs. The form taken by this cooperative oxygen effect has been discussed in the literature, and at least includes a significant component due to lateral interactions between adsorbed nitrogen and oxygen atoms on the surface. Such a contribution has indeed been justified experimentally (11) and simulated with several computer algorithms (18–20). We included this effect in our simulations and came up with an average value of about 5.4 kcal/(mol · ML) for the pairwise repulsion. Unfortunately, such interactions alone cannot entirely explain either the appearance of two N_2 peaks in the TPD or the isothermal kinetics reported here, among other reasons because similar behavior is seen on nitrogen-covered surfaces in the absence of any oxygen (16, 22).

This brings us to our last important point concerning the kinetics of the nitrogen recombination reaction, namely, that no acceptable fit to the isothermal kinetic data could be obtained without relaxing our initial hypothesis that the rate law had to be proportional to the square of the atomic nitrogen surface concentration. Interestingly, allowing for the reaction order to vary during the fit led to the estimation of a reaction rate order below unity (Fig. 9). This could be interpreted as to result from the slow diffusion of the nitrogen atoms toward each other on the surface. The derivation of an analytical expression for such a model is complicated by the fact that the coadsorbed oxygen also alters the rate of nitrogen surface mobility, but at the very least some observations can be qualitatively understood using this idea, namely:

(i) There is an induction period in the rate of molecular nitrogen formation below 600 K. This could be explained in terms of the need for a critical surface concentration of nitrogen atoms before their average interatomic distances are short enough so they can diffuse and encounter each other within a reasonable time.

(ii) That induction period becomes shorter as the surface temperature is increased. This is just because the diffusion rate, and consequently the average distance traveled per unit time, is expected to increase exponentially with temperature.

(iii) For temperatures between 450 and 550 K the rate of molecular nitrogen production is approximately proportional to the atomic nitrogen coverage in the high coverage limit, that is, in the trailing end of the isothermal kinetic runs. This is what would be expected for a two-dimensional diffusion-limited reaction, and is seen better at later times because that is the regime of high oxygen coverages where there are only small variations in the term that accounts for atomic lateral interactions.

(iv) The β_1 N_2 TPD peak temperature maximum is invariant with coverage. This is explained in the same way as in point (iii) above, that is, by assuming that the rate of atomic nitrogen diffusion is directly proportional to its coverage. It needs to be remembered that this low-temperature TPD peak is only seen for NO initial coverages above approximately 0.25 ML, a third of saturation.

To the best of our knowledge the hypothesis of N_2 production being rate-limited by atomic nitrogen surface

diffusion put forth here has not been discussed in detail before. Makeev *et al.* have recently estimated the diffusion coefficient for atomic nitrogen on Rh(111) to be $D_N = 4000\ \mu m^2/s$, the same as that for hydrogen and 3 orders of magnitude lower than those for either oxygen or NO (31). Unfortunately, their numbers were obtained by numerical modeling of complex oscillatory chemistry and appear to us to be physically unsound. Several arguments can be provided for this. First, if $D_N = D_H$, nitrogen recombination would be expected to occur at very low temperatures, below those needed for H_2 desorption from hydrogen adsorbed on Rh(111) (since the N≡N bond is so much stronger than the H–H bond). Second, there is no reason to expect D_N to be significantly different from D_O, certainly not 3 orders of magnitude larger. It only needs to be noted that the binding energies for O and N on the rhodium surface are approximately 100 and 130 kcal/mol, respectively (11, 16), so if anything nitrogen is expected to diffuse at a slower rate than oxygen (the values of diffusion barriers heights are approximately 20% of the respective binding energies). Lastly, it is logical to assume that NO molecules are much more mobile on the surface than nitrogen atoms, since their adsorption energy is so much lower (about 26 kcal/mol (11)). We believe that the estimate of D_N needs to be revised, but it is nevertheless quite clear that more isothermal kinetic experiments need to be performed to decouple the effect of lateral interactions with oxygen from that due to the nitrogen diffusion. This can be done by performing NO uptake isothermal experiments on nitrogen and/or oxygen precovered surfaces, an approach that we are pursuing at the present time. It would also be useful to extend the previous computer kinetic modeling of the TPD data to include the diffusion steps.

5. CONCLUSIONS

The kinetics of the thermal decomposition of nitric oxide on Rh(111) surfaces was characterized by isothermal measurements using a collimated directional NO beam and mass spectrometry detection. NO adsorption and N_2 desorption rates could be followed simultaneously over time and later correlated with the oxygen and nitrogen surface coverages calculated via integration of those data. Below about 350 K NO adsorption is molecular and does not lead to nitrogen (or any other product) desorption. The adsorption at 100 K follows precursor-mediated kinetics, but a more Langmuir-type behavior is seen at 300 K. Neither the NO initial sticking coefficient nor its saturation coverage vary much between 100 and 700 K; they display vales around 0.75 and 0.7 ML, respectively, in that temperature range. At the other end, above approximately 700 K, both NO decomposition and N recombination steps are fast on the surface, and N_2 production is therefore rate-limited by the impinging frequency of the incoming gas-phase NO molecules (at least under the conditions of the experiments reported here).

Perhaps the most interesting kinetic regime was seen between 350 and 700 K, because in that temperature range the rate of molecular nitrogen formation does not follow that of NO consumption. An induction period is observed in the N_2 desorption trace which depends on the reaction temperature. Gas-phase nitrogen is not detected until atomic nitrogen coverages of about 0.2 and 0.1 ML are reached at 450 and 600 K, respectively, and that induction period is followed by a sharp rise in the N_2 signal which corresponds to an empirical reaction rate order on Θ_N of between 4 and 6, after which the nitrogen coverage reaches a maximum and starts to decrease again, at least below 550 K. For the same atomic nitrogen concentration, the rate of N_2 production differs significantly in the leading and trailing edges of the experiment, presumably because of the repulsive forces induced by the presence of oxygen on the surface. The best fit to the data was obtained when a rate law that included both lateral interactions and a fractional order dependence on Θ_N was used. The results were interpreted in terms of the rate-limiting step being the diffusion of nitrogen atoms across the surface right after NO dissociation and prior to atomic nitrogen recombination. In general, it was also shown here that isothermal kinetic experiments are better suited and more demanding than TPD for testing kinetic models.

ACKNOWLEDGMENTS

Funding for this research was provided by a grant from the National Science Foundation (CTS-9525761). We also thank Dr. David N. Belton for the donation of the Rh(111) single crystal and for helpful discussions.

REFERENCES

1. Rhoads, R. G., *in* "Air Pollution by Nitrogen Oxides" (T. Schneider and L. Grant, Eds.), p. 989. Elsevier, Amsterdam, 1982.
2. Farrauto, R. J., Heck R. M., and Speronello, B. K., *Chem. Eng. News.* **Sept. 7**, 34 (1992).
3. "Catalysis Looks to the Future: National Research Council Report." National Academy Press, Washington, DC, 1992.
4. "Emission Standards for Major Air Pollutants from Energy Facilities in OCED Member Countries." Report, Organization for Economic Cooperation and Development (OCED), Paris, 1984.
5. Taylor, K. C., "Automobile Catalytic Converters." Springer-Verlag, Berlin, 1984.
6. Somorjai, G. A., *J. Catal.* **27**, 453 (1972).
7. Hegedus, L. L., Summers, J. C., Schlatter, J. C., and Baron, K., *J. Catal.* **56**, 321 (1979).
8. Shelef, M., and Graham, G. W., *Catal. Rev.-Sci. Eng.* **36**, 433 (1994).
9. Bosch, H., and Janssen, F., *Catal. Today* **2**, 369 (1998).
10. Zhdanov, V. P., and Kasemo, B., *Surf. Sci. Rep.* **29**, 31 (1997).
11. Root, T. W., Schmidt, L. D., and Fisher, G. B., *Surf. Sci.* **134**, 30 (1983).
12. DeLouise, L. A., and Winograd, N., *Surf. Sci.* **159**, 199 (1985).
13. Borg, H. J., Reijerse, J. F. C.-J. M., van Santen, R. A., and Niemantsverdriet, J. W., *J. Chem. Phys.* **101**, 10052 (1994).
14. Root, T. W., Fisher, G. B., and Schmidt, L. D., *J. Chem. Phys.* **85**, 4679 (1986).

15. Kao, C.-T., Blackman, G. S., Van Hove, M. A., Somorjai, G. A., and Chan, C.-M., *Surf. Sci.* **224**, 77 (1989).
16. Belton, D. N., DiMaggio, C. L., and Ng, K. Y. S., *J. Catal.* **144**, 273 (1993).
17. Belton, D. N., DiMaggio, C. L., Schmieg, S. J., and Ng, K. Y. S., *J. Catal.* **157**, 559 (1995).
18. Borg, H., Ph.D. Thesis, Technische Universiteit Eindhoven, 1995.
19. Makeev, A. G., and Slinko, M. M., *Surf. Sci.* **359**, L467 (1996).
20. Zhdanov, V. P., *Catal. Lett.* **37**, 163 (1996).
21. Makeev, A. G., Slinko, M. M., Janssen, N. M. H., Cobden, P. D., and Nieuwenhuys, B. E., *J. Chem. Phys.* **105**, 7210 (1996).
22. Bugyi, L., and Solymosi, F., *Surf. Sci.* **258**, 55 (1991).
23. Liu, J., Xu, M., Nordmeyer, T., and Zaera, F., *J. Phys. Chem.* **99**, 6167 (1995).
24. Öfner, H., and Zaera, F., *J. Phys. Chem.* **101**, 396 (1996).
25. "Vacuum Physics and Technology" (G. L. Weissler and R. W. Carlson, Eds.), Academic Press, New York, 1979.
26. Kim, Y. J., Thevuthasan, S., Herman, G. S., Peden, C. H. F., Chambers, S. A., Belton, D. N., and Permana, H., *Surf. Sci.* **359**, 269 (1996).
27. Zaera, F., Liu, J., and Xu, M., *J. Chem. Phys.* **106**, 4204 (1997).
28. Kisliuk, P., *J. Phys. Chem. Solids* **3**, 95 (1957).
29. van Hardeveld, M., Ph.D. Thesis, Technische Universiteit Eindhoven, 1997.
30. Xu, H., and Ng, K. Y. S., *Surf. Sci.* **365**, 779 (1996).
31. Makeev, A. G., Janssens, N. M. H., Cobden, P. D., Slinko, M. M., and Nieuwenhuys, B. E., *J. Chem. Phys.* **107**, 965 (1997).